

Table W1. Immunopathologic Table of Forty-Six Breast Cancer Tissues (IDC, Infiltrating Ductal Carcinoma; ILC, Infiltrating Lobular Carcinoma) from Primary Tumors, Matched Lymphovascular Tumor Emboli (LVI), and Axillary Lymph Node Metastases.

Age	Histotype	LVI	Diameter (mm)	pT	pN	pNcod	No. LN Pos	G	NG	IL-6 Mas	IL-6 Fr	IL-6 LVI	IL-6 LN
46	IDC	No	20	T1	N1	Pos	1	G2	NG2	1	1	1	
72	IDC	No	18	T1	N2	Pos	5	G2	NG3	0	2		2
73	IDC	Yes	25	T2	N3	Pos	10	G2	NG2	2	3	4	3
58	IDC	Yes	15	T1	N2	Pos	7	G3	NG3	2	3	4	4
85	ILC	No	15	T1	N1	Pos	2	G1	NG2	2	2		1
62	IDC	No	17	T1	N3	Pos	16	G3	NG3	2	3		3
71	IDC	Yes	20	T1	N1	Pos	1	G2	NG2	0	0	0	
92	IDC	No	14	T1	N0	Neg	0	G1	NG2	1	1		
58	IDC	No	20	T1	N0	Neg	0	G3	NG3	1	1		
83	IDC	No	18	T4				G1	NG2	0	1		
83	IDC	No	12	T1	N3	Pos	16	G2	NG3	3	4		3
63	IDC	No	30	T2	N2	Pos	5	G3	NG3	2	4		2
55	IDC	Yes	15	T1	N0	Neg	0	G3	NG3	2	2		
59	IDC	Yes	10	T1	N0	Neg	0	G3	NG3	2	3		
44	IDC	No	10	T1	N0	Neg	0	G1	NG2	0	0		
59	IDC	Yes	20	T1	N1	Pos	3	G2	NG2	0	2	2	2
39	IDC	Yes	40	T2	N3	Pos	34	G2	NG3	2	4	4	3
71	IDC	No	25	T2	N1	Pos	1	G1	NG2	0	1		
73	ILC	No	6	T1	N2	Pos	9	G2	NG3	0	0		0
73	IDC	Yes	20	T1	N1	Pos	1	G2	NG3	0	1	2	
85	IDC	Yes	25	T2	N1	Pos	2	G3	NG3	1	3	3	2
79	IDC	Yes	25	T4	N1	Pos	3	G2	NG2	1	2		
78	IDC	Yes	30	T2	N3	Pos	13	G3	NG3	2	4	4	4
55	IDC	No	11	T1	N0	Neg	0	G1	NG2	1	2		
82	IDC	No	40	T2	N1	Pos	1	G2	NG3	0	0		
61	IDC	No	25	T2	N0	Neg	0	G2	NG3	0	0		
66	IDC	No	25	T2	N0	Neg	0	G3	NG3	1	2		
76	IDC	Yes	20	T1	N1	Pos	3	G3	NG3	1	3	4	3
71	IDC	No	10	T1	N0	Neg	0	G1	NG1	0	1		
76	ILC	Yes	10	T1				G2	NG2	0	1	1	
70	IDC	Yes	37	T2	N0	Neg	0	G3	NG3	0	1	1	
66	IDC	No	40	T2	N0	Neg	0	G3	NG3	0	0		
64	IDC	Yes	12	T1	N0	Neg	0	G3	NG3	0	0		
40	IDC	No	15	T1	N1	Pos	3	G3	NG3	0	1	2	2
81	IDC	Yes	25	T2	N3	Pos	30	G3	NG3	1	3	4	3
51	ILC	No	13	T1	N0	Neg	0	G2	NG2	0	1		
63	IDC	No	30	T2	N0	Neg	0	G3	NG3	0	1		
39	IDC	Yes	20	T1	N2	Pos	4	G3	NG3	2	4	3	3
73	ILC	No	24	T2	N0	Neg	0	G2	NG2	1	2		
74	IDC	No	20	T1	N0	Neg	0	G2	NG3	0	0		
73	IDC	No	10	T1	N0	Pos	0	G2	NG3	0	2	2	
86	IDC	Yes	15	T1	N0	Neg	0	G3	NG3	0	1	2	
47	IDC	No	25	T2	N1	Pos	1	G3	NG3	1	1	2	
57	IDC	Yes	20	T1	N1	Pos	2	G2	NG3	1	2	2	2
57	IDC	Yes	70	T3	N3	Pos	15	G3	NG3	2	4	3	3

Age, primary tumor diameter, pTN, grade (G), nuclear grade (NG), and IL-6 scoring are also reported [mass, tumor front (Fr), lymphovascular tumor emboli (LVI), and lymph nodes (LN)]. Cytoplasmic IL-6 Score System: <1% = 0; 1% to 10% = 1; 10% to 25% = 2; 25% to 50% = 3; >50% = 4.

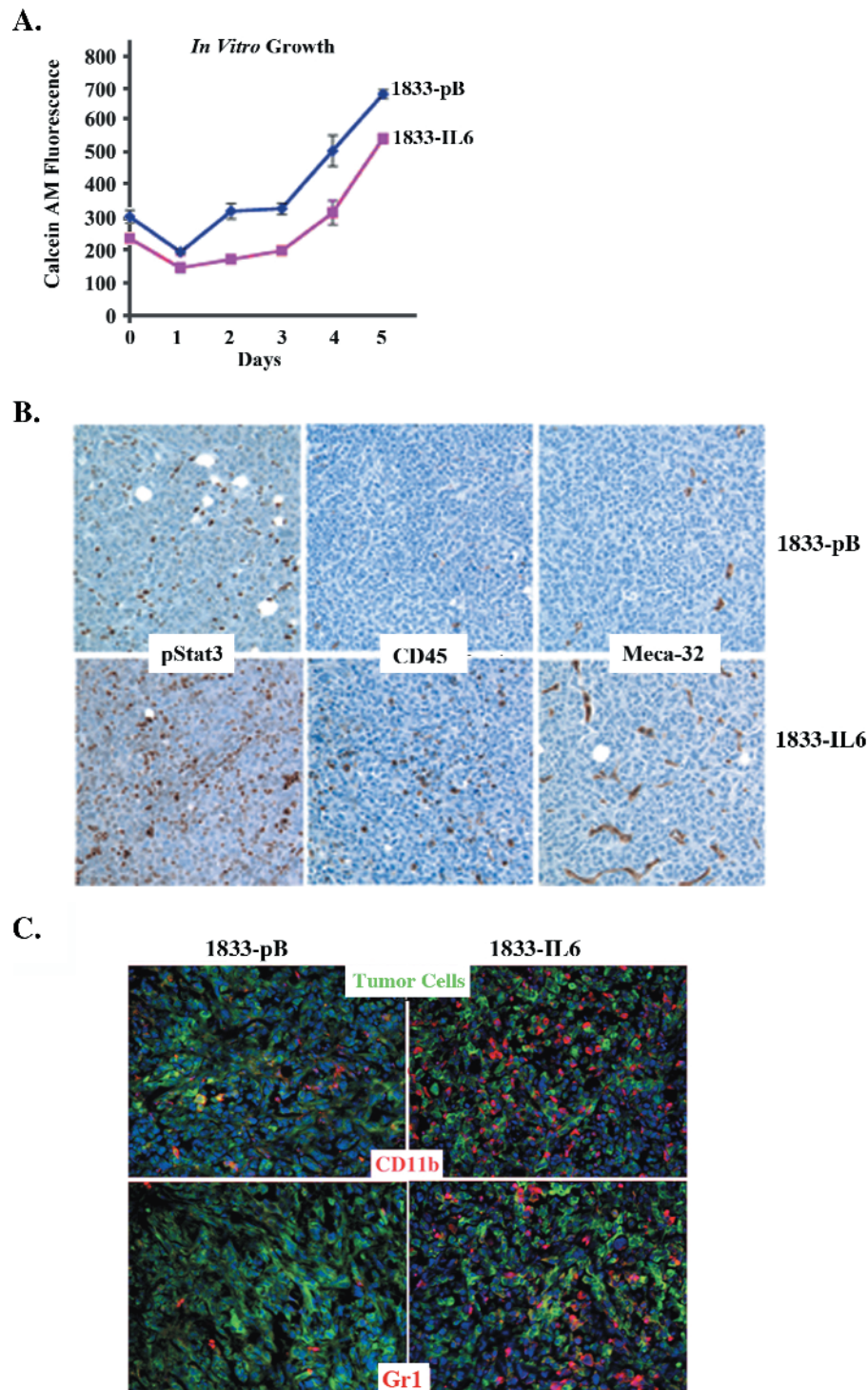


Figure W1. Comparison of 1833-pB and 1833-IL-6 cells/tumors. (A) *In vitro* growth. Equal numbers of 1833-pB and 1833-IL-6 cells were grown, and cell viability was determined daily using calcein AM fluorescence. Values are expressed as the mean of triplicates. No differences in growth rates were observed. (B) Representative histologic images of 1833-pB and 1833-IL-6 MFP tumor sections stained for pStat3, CD45, and Meca-32. (C) Representative IF images for CD11b⁺ and Gr1⁺ cells (red) found in 1833 and 1833-IL-6 (green tumor cells; blue nuclei) MFP tumors. * $P < .05$.

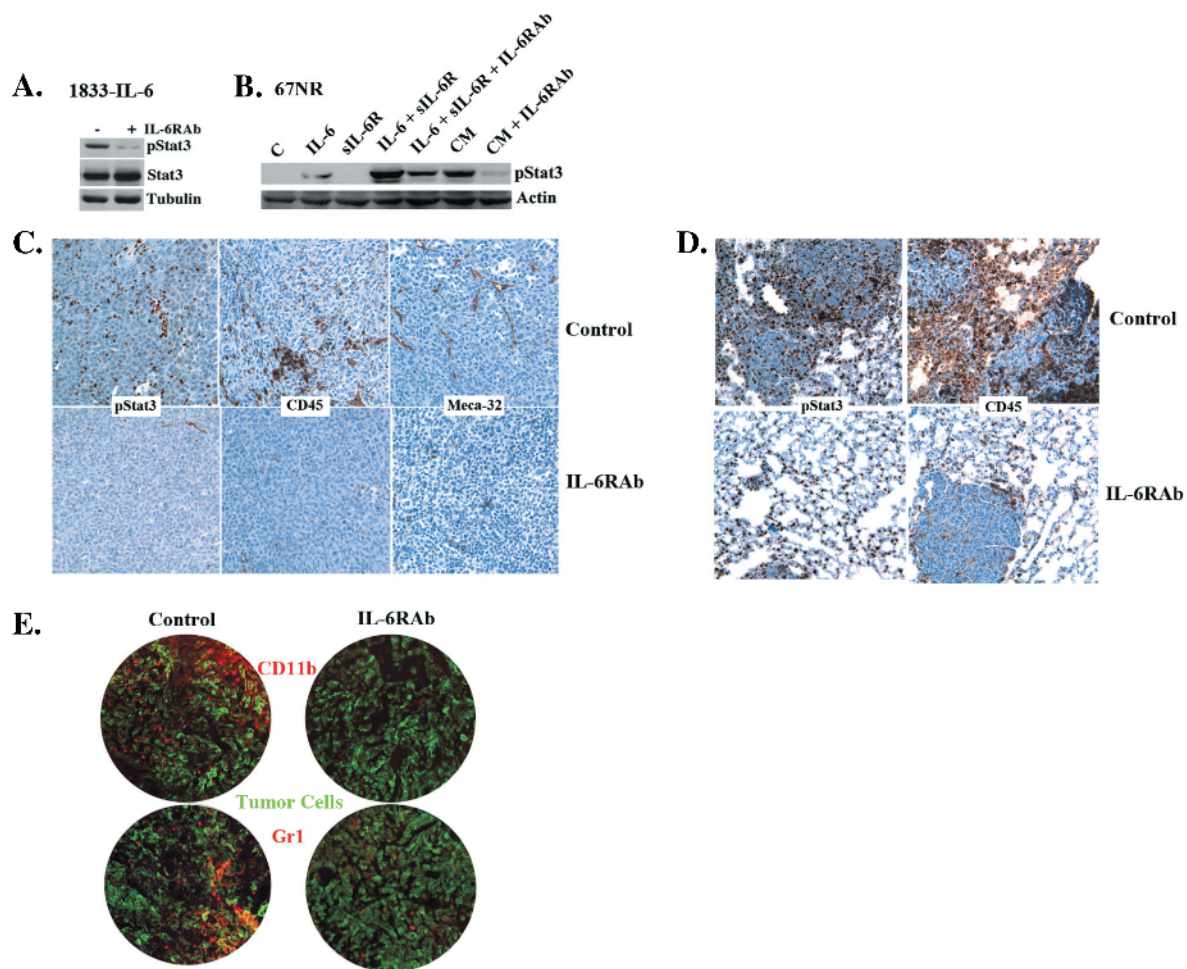


Figure W2. Consequences of IL-6R blockade. (A) Extracts from 1833-IL-6 cells treated with control IgG (–) or IL-6RAb (+) were analyzed for pStat3, Stat3, and tubulin levels by Western blot analysis. (B) Trans-signaling. Extracts from 67NR cells (murine mammary epithelial cells) treated with ligands, conditioned media, and antibodies for 2 hours [control Ab (C), IL-6, sIL-6R, IL-6 + sIL-6R, IL-6 + sIL-6R + IL6RAb, conditioned media from 1833-IL-6 cells (CM), and CM + IL-6Rab] were analyzed for pStat3 and actin by Western blot analysis. (C) Representative histologic images of MFP tumors and (D) lung sections from 1833-IL-6-injected mice treated with control antibody (C) or IL-6R antibody (IL-6RAb) stained for pStat3, CD45, and Meca-32. (E) Representative IF images of CD11b⁺ and Gr1⁺ cells (red) from mice bearing 1833-IL-6 MFP tumors (green) treated with isotype control and IL-6RAb.

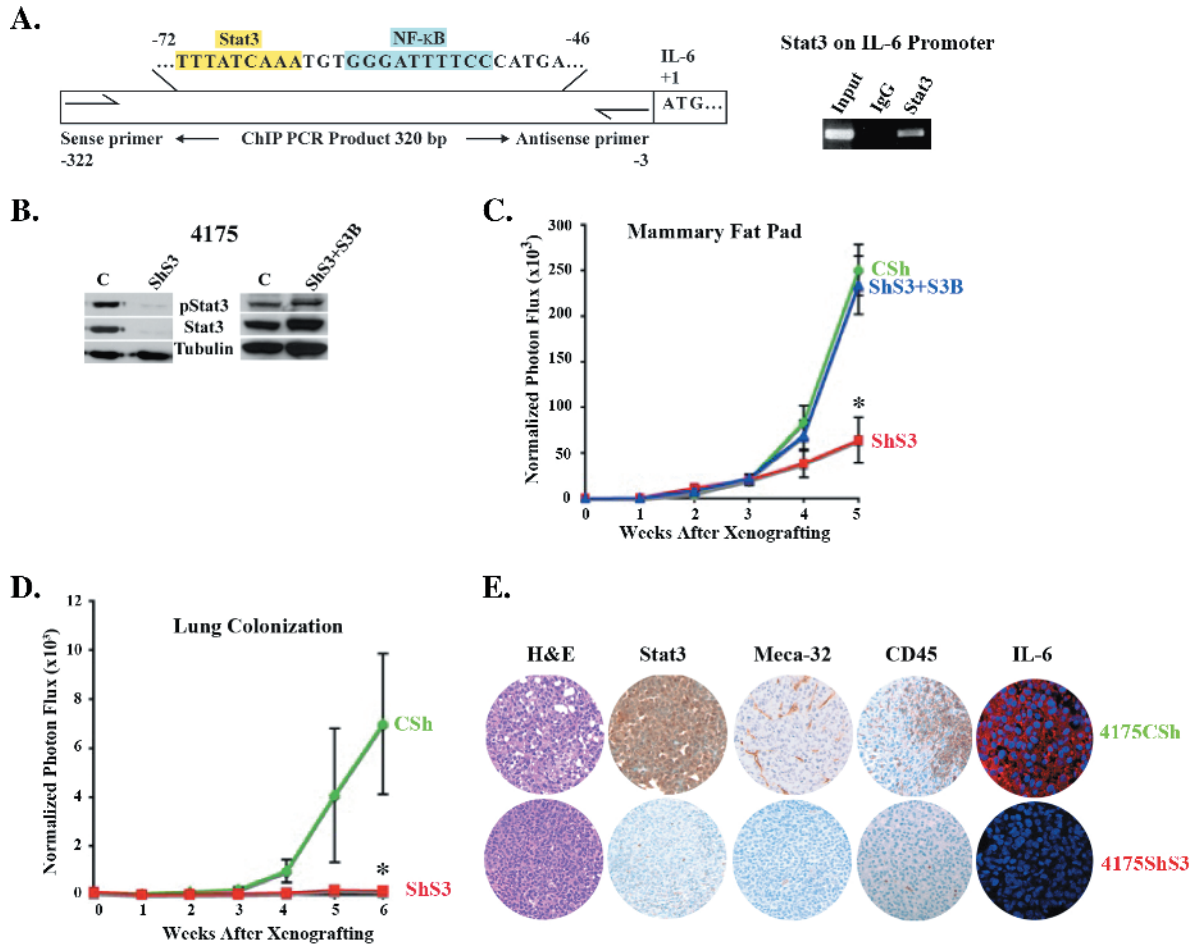


Figure W3. Stat3 regulates tumor growth. (A) A schematic of the IL-6 promoter with a putative Stat3 binding site in yellow and a canonical NF- κ B binding site in blue. Primer binding sites are indicated at -322 and -3 from the ATG. 4175 cells were subjected to ChIP assay using antibodies to Stat3 (S3) or IgG as a negative control. Co-precipitated DNA was amplified by PCR using primers flanking the Stat3 binding sites at -322 and -3 of the IL-6 promoter. The input was 5% of the total. (B) Stat3-shRNA lentiviral construct (ShS3) and control vector (CSh) were introduced into the 4175 cells. Human Stat3 was introduced into ShS3 cells (ShS3 + S3). Extracts were isolated from these and analyzed for pStat3, Stat3, and tubulin. (C) 4175 Control, ShS3, and ShS3 + S3B cells (1×10^6) were injected into the MFP, and tumor growth was determined weekly by normalized BLI ($n = 6$ mice/group). (D) 4175 Control and ShS3 cells (1×10^6) were injected intravenously leading to lung colonization, and metastatic growth was determined weekly by normalized BLI ($n = 6$ mice/group). (E) Representative histologic images of 4175 and 4175ShS3 MFP tumor sections stained for H&E, Stat3, Ki67, Meca-32, CD45, and IL-6. * $P < .05$.

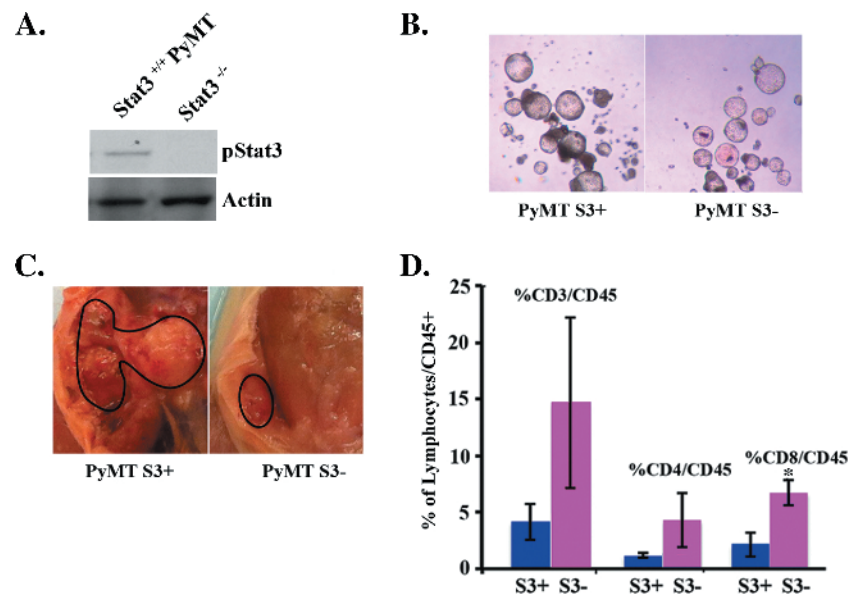


Figure W4. Tumor-extrinsic effects of Stat3 deficiency. (A) Extracts from Stat3^{-/-} and Stat3^{+/+} PyMT tumor-derived cell lines were analyzed for pStat3 and tubulin. (B) Representative light microscopy images of mammospheres cultured from PyMT S3⁺ and PyMT S3⁻ tumors. (C) Representative images of PyMT S3⁺ and PyMT S3⁻ MFP tumors. (D) The proportion (%) of CD3⁺, CD4⁺, and CD8⁺ cells in S3⁺ and S3⁻ tumors was determined by flow cytometry ($n = 5$). * $P < .05$.